

Automatic recognition of vertebral landmarks in fluoroscopic sequences for analysis of intervertebral kinematics

P. Bifulco¹ M. Cesarelli¹ R. Allen² M. Sansone¹ M. Bracale¹

¹University of Naples "Federico II", Biomedical Engineering Unit, Department of Electronic Engineering and Telecommunications, Napoli, Italy

²University of Southampton, Institute of Sound and Vibration Research, Southampton, UK

Abstract—Intervertebral kinematics closely relates to the functionality of the spinal segments. Direct measurement of the intervertebral kinematics *in vivo* is very problematic. The use of a fluoroscopic device can provide continuous screening of the lumbar tract during patient spontaneous motion, with an acceptable, low X-ray dose. The kinematic analysis is intended to be limited to planar motion. Kinematic parameters are computed from vertebral landmarks on each frame of the image sequence. Landmarks are normally selected manually in spite of the fact that this is subjective, tedious to perform and regarded as one of the major contributors to errors in the computed kinematic parameters. The aim of this work is to present an innovative method for the automatic recognition of vertebral landmarks throughout a fluoroscopic image sequence to provide an objective and more precise quantification of intervertebral kinematics. The recognition procedure is based upon comparing vertebral features in two adjacent frames by means of a cross-correlation index, which is also robust despite the low signal-to-noise ratio of the lumbar fluoroscopic images. To provide a quantitative assessment of this method a calibration model was used which consisted of two lumbar vertebrae linked by a universal joint. The reliability and accuracy of the kinematic measurements have been investigated. The errors are of the order of a millimetre for the localisation of the intervertebral centre of rotation and tenths of a degree for the intervertebral angle. Error analysis suggests that this method improves the accuracy of the intervertebral kinematic calculations and has the potential to automate the selection of anatomical landmarks.

Keywords—Intervertebral kinematics, Vertebral segments, Motion analysis, Fluoroscopy, Time-varying image processing

Med. Biol. Eng. Comput., 2001, 39, 65–75

1 Introduction

THE MECHANICAL functionality of the spine depends on the dynamic behaviour of its components; the vertebrae, the discs and the ligaments, in conjunction with the actions of the muscles. Spinal functional alterations and related pathologies generate various disabilities, constituting a widespread problem, which continues to grow. Due to the natural inaccessibility and the complex structure of the spinal segments, *in vivo* measurements of their mechanics are very problematic. Intervertebral kinematics closely relates to the state of the individual spinal segments and then to spine functionality. Research on intervertebral motion has, therefore, been widely regarded as an essential prerequisite to improve the knowledge of the mechanics of the spine and its disorders.

Since WEBER (1827), spinal motion has been widely investigated. Most of the analyses to characterise the intersegmental motion of the vertebral column *in vivo* were carried out using

plain radiography. TODD and PILE (1928) and BAKKE (1931) first reported the use of X-ray images. These techniques were improved by GIANTURCO (1944) and TANZ (1953), who measured the angles between vertebral bodies at the extreme trunk range in normal and symptomatic (back pain) subjects. More accurate and exhaustive kinematic studies were carried out *in vitro* using cadaveric spinal segments. These studies provided a 3D characterisation of the segmental motion of the lumbar (ROLANDER, 1966), thoracic (WHITE, 1969) and cervical (LYSELL, 1969) spine. Full 3D motion analysis *in vivo* has been attempted using biplanar radiographic equipment since the work of BROWN *et al.* (1976). More reliable 3D kinematic intersegmental data can be obtained *in vivo* by means of insertion of pins in the vertebrae (STEFFEN *et al.*, 1997) (generally utilised only for pre-operative analysis, e.g. implantation of spinal fixators).

The possibility of using non-invasive methods such as flexible rules, inclinometers and goniometers or skin optical markers has been widely considered. However, these methods provide reliable information only about the movement of an entire section of the spine rather than about individual segments. Skin and soft tissue effects also impede reliability of surface measurements although for routine, gross assessment, such methods can be useful in the clinic.

Correspondence should be addressed to Dr P. Bifulco;
email: bifulco@diesun.die.unina.it

First received 5 May 2000 and in final form 9 October 2000

MBEC online number: 20013545

© IFMBE: 2001

Most of the *in vivo* studies employing conventional radiography, perform end-of-range measurements, or analyse a very few finite steps of motion (DIMNET *et al.*, 1978; PEARCY and BOGDUK, 1988). The number of exposures that can be obtained from one subject (CHOLEWICKI and MCGILL, 1992) is very limited to maintain radiation at an acceptable level and, in addition, only static images are produced. From a diagnostic point of view, not only the extremes of movements, but also the motion pattern in between, is of interest and can indicate underlying pathology (PEARCY, 1986). Several relationships between vertebral motion patterns and disability have been plausibly hypothesised, but few have been proven. Some evidence has been offered, relating excessive intervertebral translation to both disc degeneration (GERTZBEIN *et al.*, 1985; AN *et al.*, 1996) and pain (FRIBERG, 1987).

Recently, the use of fluoroscopy has been proposed by different authors to study *in vivo* intervertebral kinematics. This technique allows a more continuous motion analysis, and can provide useful diagnostic data, maintaining radiation exposure low enough to be acceptable for clinical application. The use of a single fluoroscopic device, readily available in the clinical environment, could allow routine analysis to be carried out. Work by CHOLEWICKI *et al.* (1991), CHOLEWICKI and MCGILL (1992), BREEN *et al.* (1993), investigated lumbar motion, while VAN MAMEREN (1988), VAN MAMEREN *et al.* (1990, 1992), PAGE and MONTEITH (1992), PAGE *et al.* (1993), AMEVO (1991) and AMEVO *et al.* (1991), concentrated their attention on the cervical spine. The use of a single fluoroscopic device limits analysis to planar motion of the spine. This assumption is reasonable in some cases, as PEARCY (1986) reported (see also PANJABI and WHITE, 1971; PANJABI, 1973; PEARCY *et al.*, 1984; and PEARCY and TIBREWAL, 1984). Although flexion-extension movements generally occur without significant lateral bending or axial rotation (i.e. coupled motion) this is not case for lateral bending. However, even if, for the lateral bending of the lumbar tract, the amount of coupled motion is relatively small with respect to the other tract, only the flexion-extension in sagittal plane can be assumed to be a planar motion.

From a fluoroscopic sequence of images of the spine, a kinematic description of motion is based upon features of the vertebrae observed throughout the frames. A variety of different features or landmarks (e.g. vertebral body edges or corners, processes or pedicles) and measurement techniques have been proposed. For kinematic analysis the hypothesis of rigidity must hold for the vertebrae. Such an assumption is natural since deformation of the vertebrae caused by the forces acting on the vertebral column during motion are negligible with respect to the displacement involved FRANKEL and BURSTEIN (1974). A range of kinematic indices have been reported in the literature to describe motion and among these are intervertebral angles, axis of motion (FICK and STRASSER, 1913), instantaneous centre of rotation (ICR) (DITTMAR, 1929) and helical axis of motion (PANJABI and WHITE, 1971; KINZEL *et al.*, 1972). A biological significance has been proposed (BOGDUK *et al.*, 1995) for the ICR as a function of the centre of the reaction force of a vertebra.

For a reliable study of intervertebral kinematics, accurate measurements of the vertebrae positions throughout a motion sequence are required. This is due to the relatively small range of motion of individual vertebral units and intrinsic errors in the computation of the kinematic parameters (PANJABI, 1979; PANJABI *et al.*, 1992). Nevertheless, manual intervention VAN MAMEREN *et al.*, 1990, 1992; BREEN, 1991; BREEN *et al.*, 1993; SIMONIS, 1994) is still largely used for vertebral landmark identification in spite of the fact that it is regarded as one of the major contributors to errors (PANJABI *et al.*, 1992). Moreover, the low X-ray dosage adopted for fluoroscopic

analysis results in poor quality image sequences which complicate the situation. This is particularly true for the lumbar spine because of the larger amount of soft tissue involved.

The aim of this work is to present an innovative method for the automatic recognition of vertebral landmarks throughout a fluoroscopic image sequence to provide an objective and more precise quantification of intervertebral kinematics. The analysis has concentrated upon lumbar spine kinematics. To provide a quantitative assessment of this method, fluoroscopic sequences of a calibration model consisting of two lumbar vertebrae have been used. The recognition method is shown to be robust with respect to the high levels of noise in the images. Preliminary results are also presented for *in vivo* images.

2 Method

2.1 Instrumentation and experimental set-up

To investigate lumbar spine motion, a fluoroscope system is utilised to screen the patient's lumbar area during spontaneous movement of flexion, extension and left and right lateral bending. A schematic diagram of the system is shown in Fig. 1. Fluoroscopes equipped with a 9 or 11 inch image intensifier were used. The image intensifier was manually moved during the patient exercise to contain the lumbar area in view. The output of the intensifier was stored on videotape for subsequent off-line processing and enabled images from different centres to be assessed. Current work is, however, acquiring images directly from the intensifier in order to improve image quality.

The X-ray parameters adopted were, on average, set to 85 kV and 2 mA and the duration of the subject's movement (plus the alignment) took no more than 20 s (BREEN, 1991). To evaluate directly the radiation exposure of the patient, thermoluminescent dosimeters (BREEN *et al.*, 1993) were utilised. The absorbed X-ray dose for 10 s screening was 3 mGy for antero-posterior views and 13 mGy for lateral views. For comparison it is useful to remember that the entry dosage of a conventional plain

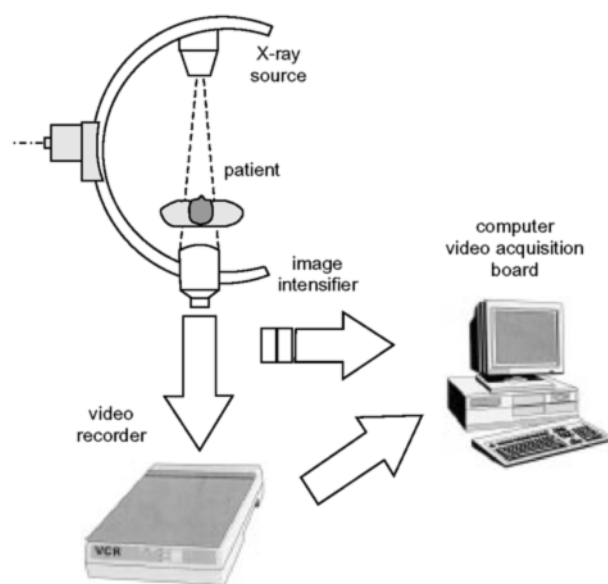


Fig. 1 Instrumental set-up: the output of the monitor of the fluoroscopic device is connected to a video recorder. The bending movements are recorded on videotape. Sequences of images are then sequentially grabbed (by means of the PC acquisition board) from the video recorder output. In future, dynamic images will be acquired directly from the fluoroscopic device

radiograph of the lumbar spine is about 20 mGy for an antero-posterior view and 50 mGy for a lateral view (PEARCY, 1985).

The videofluoroscopy device was connected to an Umatic video recorder to store the image sequences on videotape. The single images are sequentially digitised using a PC video frame-grabber board.* The size of a digital image is typically 512 by 512 pixels, while the image intensity is quantised to 256 grey levels. The images are corrected to minimise distortion (BREEN *et al.*, 1989, 1993). The maximum spatial resolution achieved is 0.25 mm by 0.25 mm per pixel. When possible, consecutive frames were time averaged to increase signal-to-noise ratio (SNR).

2.2 Vertebral anatomical landmarks

Motion estimation is performed from features, or landmarks, on the vertebrae observed throughout an image sequence (a classical problem in computer vision) (HUANG and NETRAVALI, 1994). A variety of different features can be considered such as points, lines and corners. In our case the four points corresponding to the corners of the imaged body of the vertebra were chosen as landmarks (Fig. 2). They are the more obvious features of the vertebral body projection and have already been employed by several authors (BREEN, 1991; BREEN *et al.*, 1993; CHOLEWICKI *et al.*, 1991; SIMONIS, 1994). Moreover, if the vertebral body is considered to approximate a cylinder (DIMNET *et al.*, 1978), its projection on the radiographic plane is almost invariant for small, out-of-plane rotations. Consequently, these landmarks have the advantage of relative insensitivity to coupled motion (i.e. axial rotation). VAN MAMEREN *et al.* (1990, 1992), in addition, utilise a fifth landmark placed on the extremity of the posterior process in sagittal plane images of the cervical spine, but this landmark is clearly not visible in lumbar images. It is worth mentioning that the vertebra endplate contours, still visible even in very noisy images, can be considered as alternative or integrate features (AUBIN *et al.*, 1998).

2.3 Automatic landmark recognition by means of cross-correlation

Previous studies on the subject (VAN MAMEREN, 1988; BREEN, 1991; SIMONIS, 1994) utilised manual identification of the anatomical landmarks throughout the sequence. For each frame, the operator was required to locate by hand the vertebral landmarks, utilising a pointer device combined with a display system. This operation results in a subjective, tedious and often insufficiently accurate procedure. In fact, kinematic calculation suffers from an intrinsic problem: large errors in the computation of kinematic parameters may result from relatively small errors in the identification of the spatial landmark co-ordinates (PANJABI, 1979). Manual intervention, in particular, is regarded as a major contributor to errors (PANJABI *et al.*, 1992).

In an attempt to overcome these drawbacks, an automatic process of vertebral position recognition has been implemented. It consists of tracking the vertebral landmarks (selected in the first frame) along the image sequence, recognising image features associated with the landmarks by means of cross-correlation (Fig. 3). The use of the cross-correlation provides an effective estimation of position combined with a degree of independence from noise. Through a sequence, parts of an image are held as a template which is compared with the next image in the sequence by means of the cross-correlation index. The estimation of a template position in the next frame is derived by locating the maximum value of the index.

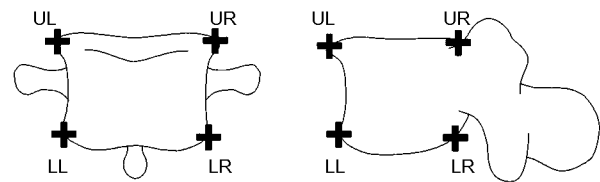


Fig. 2 Vertebral landmarks adopted in this study. They are labelled as: UL – upper left, UR – upper right, LL – lower left, LR – lower right

The image sequences obtained by fluoroscopic devices can show large variations in brightness and contrast between frames, and even locally within a single image. This is due to elements such as poor positioning of the subject, subject motion or automatic gain control of the fluoroscope (i.e. the flare effect). These changes have been found not to influence the ability to manually identify vertebrae (BREEN *et al.*, 1993), but they require consideration for automatic processing.

The expression of the cross-correlation can be formulated in order to be insensitive to both contrast and brightness variations. The effect of local image contrast can be removed by using a normalised expression of the cross-correlation (as in eqn 1). The variations of brightness (that between frames can be considerable) can be compensated for using a mean-centred cross-correlation (i.e. by filtering or subtracting the DC component of the images).

Assuming that the matrix T represents the template and M an equally-sized part of the subsequent image, centred on co-ordinates (m, n) , the normalised and mean-centred cross-correlation $r(m, n)$ can be expressed as

$$r(m, n) = \frac{\sum_{i,j} T_{AC}(i, j) \cdot M_{AC}(i + m, j + n)}{\sqrt{\sum_{i,j} T_{AC}^2(i, j) \cdot \sum_{i,j} M_{AC}^2(i + m, j + n)}} \quad (1)$$

where the subscript AC indicates that the mean brightness value has been subtracted from the images and subscripts i and j are selected to cover the whole image.

From a qualitative point of view the cross-correlation could be regarded as a 'similarity' index. Hence, the cross-correlation maximum locates the part of the subsequent image most similar to the template. In addition, the cross-correlation, due to its nature, has the advantage of being rather insensitive to additive noise. A similar, but more rudimentary, technique was proposed by PAGE and MONTEITH (1992) and PAGE *et al.* (1993) for analysing cervical spine kinematics in the sagittal plane.

Computation of the cross-correlation between two images requires a considerable amount of time. However, the operation of cross-correlation can be equivalently performed in the frequency domain with a reduction in computation time (BIFULCO, 1998). Considering a matrix of size N by N representing the current image and a matrix of size P by P representing the template, the number of operations required for cross-correlation in the spatial domain (considering the numerator of eqn 1) is approximately given by $N^2 \cdot P^2$ while in the frequency domain (JAIN, 1989) it is approximately $N^2(3 \log_2 N + 4)$.

2.4 The recognition procedure

2.4.1 Template definition: On the first frame of the sequence the operator selects the four landmarks on the vertebral body corners, for each vertebra to be examined (Section 2.2). For each vertebra, using the selected landmark co-ordinates, a main template, including the entire vertebral body and four small corner templates surrounding each landmark, are automatically generated (Fig. 4). The templates can be manually adjusted to exclude structures not rigidly connected to the vertebra (e.g. adjacent vertebrae).

* Optimas Ltd.

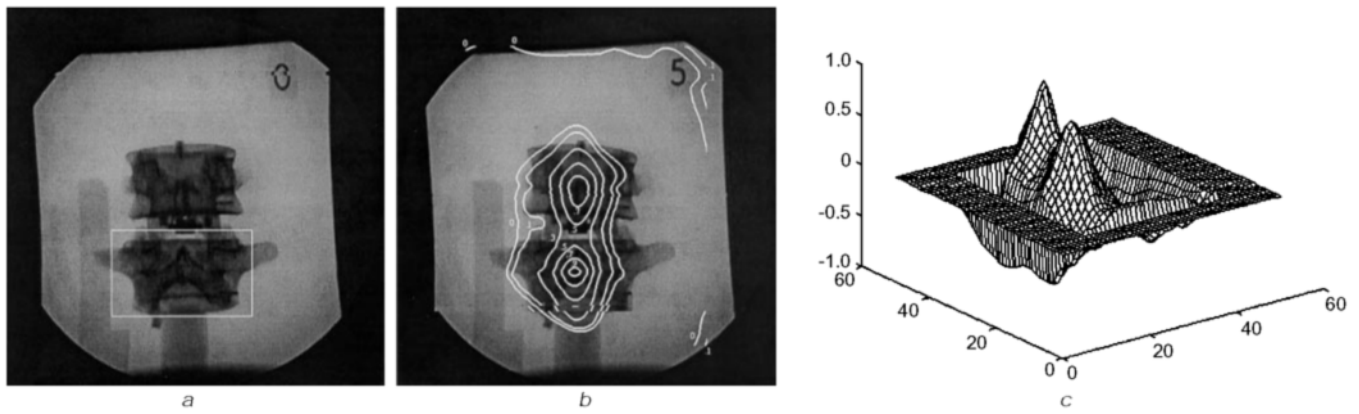


Fig. 3 Example of cross-correlation (isopleth curves and mesh). (a) The template used to locate the vertebra position on the subsequent image is represented as a white rectangle (around L4). (b) The result of cross-correlation with the template is represented as isopleth curves superimposed onto the subsequent image. A clear maximum appears on the centre of the L4 vertebra. (c) The cross-correlation is also represented as a mesh 3D plot

The main vertebral template is utilised for a preliminary estimation of the location of the vertebra in the next image. The four small corner templates are then utilised to precisely locate the vertebral landmarks from which the vertebral position can be estimated and the kinematics computed. Note that the templates constitute all the information we know about the vertebral shape, without assuming any *a priori* knowledge.

2.4.2 Approximate vertebral location: First, an approximate, preliminary location is estimated using the vertebral template and the next image in the sequence. Comparing the main template with the image, the new position of the vertebral centre is estimated by the maximum cross-correlation value. Obviously, the location obtained is only approximate, since the vertebra may have rotated between the two frames. Consequently the cross-correlation is recomputed around the estimated centre, rotating the main template progressively in 1° increments. The idea is to find, from successive attempts, the rotation of the template that maximises the likelihood of a match with the image. The cross-correlation maxima, found for each increment, constitute a series. Fig. 5 illustrates a typical course of the cross-correlation maxima against progressive test angles. The procedure is iterated until a maximum is reached for this series. The procedure is totally automated and is based on a gradient-driven search. The angle corresponding to the absolute maximum is taken as a rough estimation of vertebral rotation. In addition, the co-ordinates of the vertebral centre are refined and a simple variation of this method can be found in MUGGLETON and ALLEN (1997).

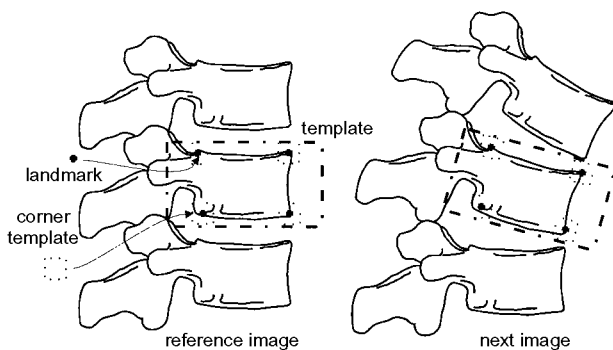


Fig. 4 Use of templates for the recognition procedure. On the right is shown a schematic representation of the templates associated with a single vertebra. The main template (---) surrounds the vertebral body and the four corner templates (···) surround the vertebral landmarks (+, +)

This procedure leads to an overall vertebral location within an image, but the displacement and rotation obtained are approximate and cannot be used to compute accurate kinematics (BIFULCO, 1998). In fact, the soft tissue does not move rigidly with the vertebrae, changing its contribution to the vertebra projection. No precautions have been taken to exclude out-of-plane motion effects. In addition, the template rotation increment is limited by the interpolation required for the image rotation.

2.4.3 Location of anatomical landmarks: Since we require an accurate identification of the four landmarks, further cross-correlation is carried out involving, separately, the four corner templates (Fig. 4). The recognition process is carried out within a limited area around their expected positions obtained from the approximate vertebral location computed previously. For the recognition procedure, the four corner templates are rotated to the vertebral angle estimated.

2.4.4 Restoration of rigidity to landmarks: The hypothesis of rigidity is maintained for the vertebrae for kinematic analysis. Such an assumption is legitimised by the fact that the deformations of the vertebrae, caused by the forces acting on the vertebral column during motion, are negligible with respect to the displacement involved (FRANKEL and BURSTEIN, 1974).

The landmark co-ordinates detected, being independent estimations, do not respect the assumption of rigidity held for the vertebra (SIMONIS *et al.*, 1994). Rigidity is restored to re-establish mutual landmark distances (BIFULCO *et al.*, 1997). The problem can be regarded as placement of the rigid structure

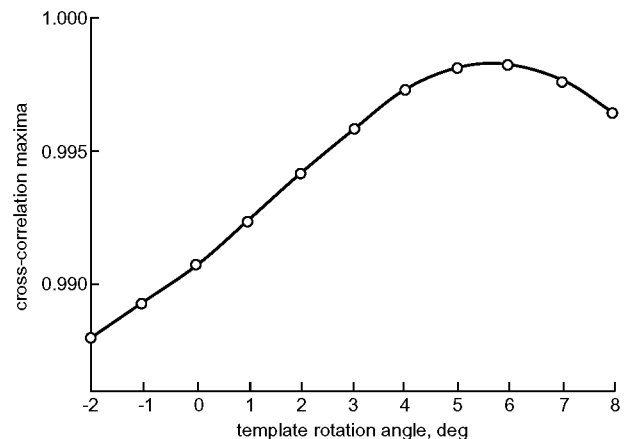


Fig. 5 An example of a typical sequence of cross-correlation maxima against progressive test angles. The angle corresponding to the absolute maximum is used to estimate the amount of vertebral rotation

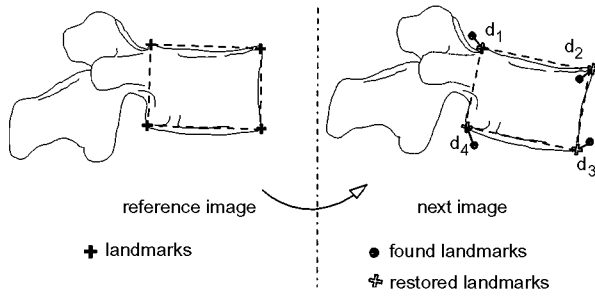


Fig. 6 Restoration of rigidity to the vertebral landmarks. The landmarks found in the next images are restored to preserve the rigid structure in the reference image (by minimising the sum of the square distances).

formed by the landmarks in the reference image onto the next frame. The detected landmarks, even if they are non-rigid, are considered to be good estimators of the correct position. The problem is then to place the landmarks' rigid structure as close as possible to those detected (Fig. 6).

A criterion to mathematically express the requirement is that of minimising a function of the distances from these points. An optimum solution can be found by minimising the sum of the squared distances:

$$\min \left\{ \sum_{i=1}^4 d_i^2 \right\} \quad (2)$$

This can be expressed by translating the centroid of the rigid reference landmarks structure onto the centroid (B_x, B_y) of the non-rigid, identified landmarks and rotating the rigid structure by an angle θ , as in the equations

$$B_x = \frac{1}{4} \sum_{i=1}^4 F_{ix} \quad B_y = \frac{1}{4} \sum_{i=1}^4 F_{iy} \quad (3)$$

$$\tan(\theta) = \frac{\sum_{i=1}^4 (\bar{L}_{ix} \bar{F}_{iy} - \bar{L}_{iy} \bar{F}_{ix})}{\sum_{i=1}^4 (\bar{L}_{ix} \bar{F}_{ix} + \bar{L}_{iy} \bar{F}_{iy})} \quad \begin{aligned} \bar{L}_i &= \left(L_i - \frac{1}{4} \sum_{i=1}^4 L_i \right) \\ \bar{F}_i &= \left(F_i - \frac{1}{4} \sum_{i=1}^4 F_i \right) \end{aligned} \quad (4)$$

where L identifies the original landmarks (reference image) while F identifies the newly found landmarks (next image), the subscript i represents each of the four landmarks, the subscript x and y indicate the components of a landmark along the X-axis and the Y-axis, respectively.

However, this solution is not robust with respect to landmarks which are erroneously identified: such circumstances can be occasionally encountered, especially for the extremes of the range of motion (where the inter-vertebral distances are reduced) or in the presence of significant levels of image noise. A mis-recognised landmark tends to move the rigid landmarks frame away from its correct position. To avoid this negative effect, a procedure based on evaluation of the maintenance of the mutual distances between landmarks has been used to reject mis-recognised landmarks (BIFULCO, 1998).

2.5 Kinematic parameters

2.5.1 Absolute kinematics: Given the vertebral landmark co-ordinates in relation to two generic frames it is possible to compute the intervertebral angle and the centre of rotation (PANJABI, 1979). These parameters totally characterise the inter-frame rigid planar motion of the vertebra. In particular, a biological basis has been proposed for the intervertebral instantaneous centre of rotation (or ICR) (BOGDUK *et al.*, 1995), being a function of the centre of the reaction forces of a vertebra with respect to its sub-adjacent neighbour. The

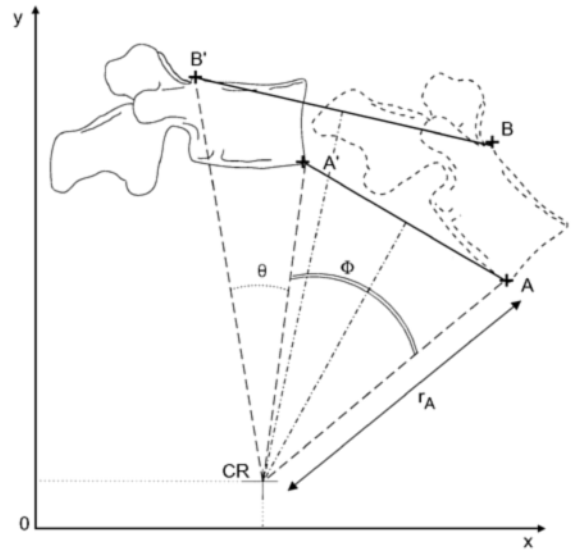


Fig. 7 Angle and centre of rotation as kinematic indices. $A(X_1, Y_1)$ and $B(X_2, Y_2)$: landmarks on the reference image; $A'(X_3, Y_3)$ and $B'(X_4, Y_4)$: landmarks on the subsequent image; ICR: centre of rotation; Φ : angle of rotation; θ : angle subtended by the two landmarks A and B at the estimated ICR (A -ICR- B); r_A : landmark distance from estimated ICR (ICR- A)

ICR constitutes the point about which the back muscles are assumed to exert their force during spine motion. Abnormal location of the ICRs is felt to be an indicator of a mechanical disorder of the segment.

The angle of rotation and the ICR are defined instantaneously. However for all practical purposes the range of motion can be divided into finite steps of motion and the centre of rotation (or CR) can be determined for each of the steps (PANJABI, 1979). In the biomechanical literature the CR and the ICR are often used interchangeably. This can be justified on the grounds that the difference between the actual location of the CR and the ICR of a joint is relatively small and decreases with reduction of the sampling time interval. Fig. 7 illustrates the situation.

The motion of a landmark (A to A' say) can be described by means of

$$\begin{pmatrix} X_3 \\ Y_3 \end{pmatrix} = \begin{pmatrix} \cos(\Phi) & -\sin(\Phi) \\ \sin(\Phi) & \cos(\Phi) \end{pmatrix} \cdot \begin{pmatrix} X_1 & -X_C \\ Y_1 & -Y_C \end{pmatrix} + \begin{pmatrix} X_C \\ Y_C \end{pmatrix} \quad (5)$$

where X_C and Y_C are the co-ordinates of the ICR and Φ is the angle of rotation.

Knowing the landmark co-ordinates in the reference image $A(X_1, Y_1)$, $B(X_2, Y_2)$ and in the next image $A'(X_3, Y_3)$, $B'(X_4, Y_4)$, the kinematic parameters ICR (X_C, Y_C) and the angle of rotation Φ can be computed. It is relatively easy to show that the solutions can be expressed by

$$\begin{aligned} X_C = & \frac{(Y_4 - Y_3) \cdot (X_2^2 - X_1^2 + Y_2^2 - Y_1^2) - (Y_2 - Y_1) \cdot (X_4^2 - X_3^2 + Y_4^2 - Y_3^2)}{2 \cdot ((X_2 - X_1) \cdot (Y_4 - Y_3) - (X_4 - X_3) \cdot (Y_2 - Y_1))} \quad (6) \end{aligned}$$

$$\begin{aligned} Y_C = & \frac{(X_2 - X_1) \cdot (X_4^2 - X_3^2 + Y_4^2 - Y_3^2) - (X_4 - X_3) \cdot (X_2^2 - X_1^2 + Y_2^2 - Y_1^2)}{2 \cdot ((X_2 - X_1) \cdot (Y_4 - Y_3) - (X_4 - X_3) \cdot (Y_2 - Y_1))} \quad (7) \end{aligned}$$

and the angle of rotation by

$$\sin(\Phi) = \frac{(X_1 - X_C) \cdot (Y_2 - Y_C) - (X_2 - X_C) \cdot (Y_1 - Y_C)}{(X_1 - X_C)^2 + (Y_1 - Y_C)^2} \quad (8)$$

Geometrically the ICR can be obtained by the intersection of the bisectors of the segments AA' and BB' , while the angle of rotation is given by A -ICR- A' as shown in Figs 7 and 8.

2.5.2 Relative kinematics: Motion is computed with respect to a reference system relative to the image frame. If the fluoroscope has not been moved between two image frames, we can consider this motion with respect to the device (absolute kinematics). To study intersegmental motion, vertebral kinematic parameters are usually computed with respect to the lower vertebra of each pair (relative kinematics). In this case, with respect to the image reference system, the motion of the lower vertebra must be compensated (Fig. 8).

As schematically shown in Fig. 8, to compute relative kinematic indices the modified landmark co-ordinates A^* and B^* , instead of A and B , have to be taken into account. These modified landmark co-ordinates A^* and B^* , are obtained by rotating and translating the landmark co-ordinates A and B using the kinematic parameters estimated for the lower vertebra. In this way all the calculations are referred to a rigid reference frame fixed on the lower vertebra (Oxy in Fig. 8). Fig. 8 shows the ICR computed relative to the lower vertebra while the rotation angle Φ can be represented by $A^* - CR - A'$ or $B^* - CR - B'$.

2.5.3 Errors in the estimation of the kinematic parameters: Previous studies by PANJABI (1972) and PANJABI *et al.* (1992) analysed the experimental errors associated with vertebral kinematic measurements. The principal factors which contribute to errors are (with reference to Fig. 7): (i) the error in the estimation of the landmark co-ordinates (A , A' , B , B'); (ii) the amplitude of the actual rotation Φ of the rigid body; (iii) the angle θ between the two landmarks from the centre of rotation ICR; (iv) the distance r of the landmarks from the centre of rotation ICR.

The first factor highlights the strong dependence of errors on the precision of the landmark co-ordinates: relatively small errors in landmark location may lead to large errors in the estimation of the kinematic parameters ICR and Φ . Therefore, accurate location of the landmarks is required while tracking motion. The second factor reminds us that for a reliable measurement of the kinematic parameters ICR and Φ to be achieved, there must be sufficient rotation in the motion (of the order of at least 5° or 6°). It is worth mentioning that for pure translation the ICR tends to infinity. The last two items suggest a preferable location, for minimisation of errors, of the landmarks with respect to the ICR: the angle θ between landmarks, seen

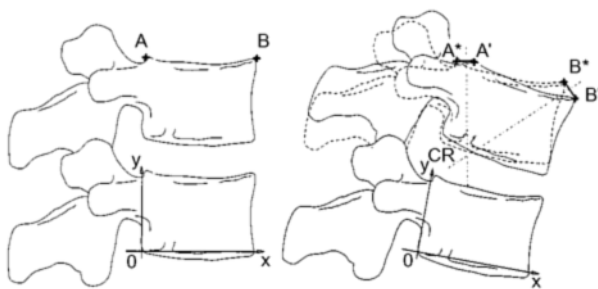


Fig. 8 Relative kinematic indices for vertebrae pairs (spinal segments). To determinate the kinematics of the upper vertebra with respect to the lower vertebra, the motion of the lower vertebra must be compensated

from the ICR, has to be large, and preferably of the order of 90° ; while the distances r of the landmarks from the CR have to be as large as possible.

2.6 Fluoroscopic sequences of a 'calibration model'

To validate the measurement method, a calibration model, already employed in previous studies (BREEN, 1991; SIMONIS, 1994), has been used. It consists of two human lumbar vertebrae (L3 and L4) linked, at the disc level, by means of a universal joint. The distance between the vertebral bodies is 8 mm. The joint allows the vertebra L3 to rotate with respect to L4, which is fixed to a support. A system of preset positions constrains the rotation of L3 with respect to L4 to known values.

Fluoroscopic image sequences of the calibration model at a range of intervertebral angles have been used to assess the reliability and accuracy of the measurements. These sequences were obtained by rotating L3 in the sagittal and in the coronal plane (without out-of-plane motion) in intervals of 5° . The value of 5° for the intervertebral rotation steps was chosen in consideration of the problems mentioned above concerning the errors in kinematic estimation. The divergence of the errors (for ICR location) has limited researchers and physicians to computing kinematic parameters only when the inter-frame motion exceeds 6° or 7° (BREEN, 1991; SIMONIS, 1994). The calibration model was not built with the aim of assessing measurement of the intervertebral angle to accuracies of the order of tenths of a degree. The preset angular positions are considered to be accurate to within $\pm 0.25^\circ$. Regarding the ICRs, the centres of all possible rotations are obviously constrained to be located in the middle of the universal joint. The metal central part of the universal joint is particularly visible in the fluoroscopic images and it appears, in both directions, as a dark rectangle in between the vertebrae (Fig. 9).

2.7 Repeatability and sensitivity of the measurement

For the experimental measurements, a repetitive calculation of kinematic parameters was performed to assess the accuracy of the method in terms of repeatability and sensitivity to the choice of landmarks manually identified in the first frame. To analyse the sensitivity of the kinematic parameters to the selection of landmarks, the entire procedure of recognition was iteratively repeated, considering as input the pixels surrounding each landmark. This simulates different operator choices during landmark selection on the first frame. For each of the four landmarks associated with a vertebra, the eight neighbouring pixels were considered as further experimental input data and were used in the pattern shown in Fig. 10.

Hence, the landmark recognition procedure is repeated 36 (4 by 9) times, resulting in four groups of nine estimated landmarks. All the landmarks found can be combined into 9^4 (6561) possible sets of four points associated with a vertebra. For each data set it is possible to perform the rigidity restoration procedure and then compute the kinematics indices. The procedure described leads to a considerable number of kinematic measurements that can be analysed statistically, allowing investigation of the possible propagation of errors in the various frames.

3 Results

3.1 Analysis of a coronal and a sagittal sequences of the calibration model

Two sequences consisting of five images of the calibration model at different intervertebral angles were used in the tests.

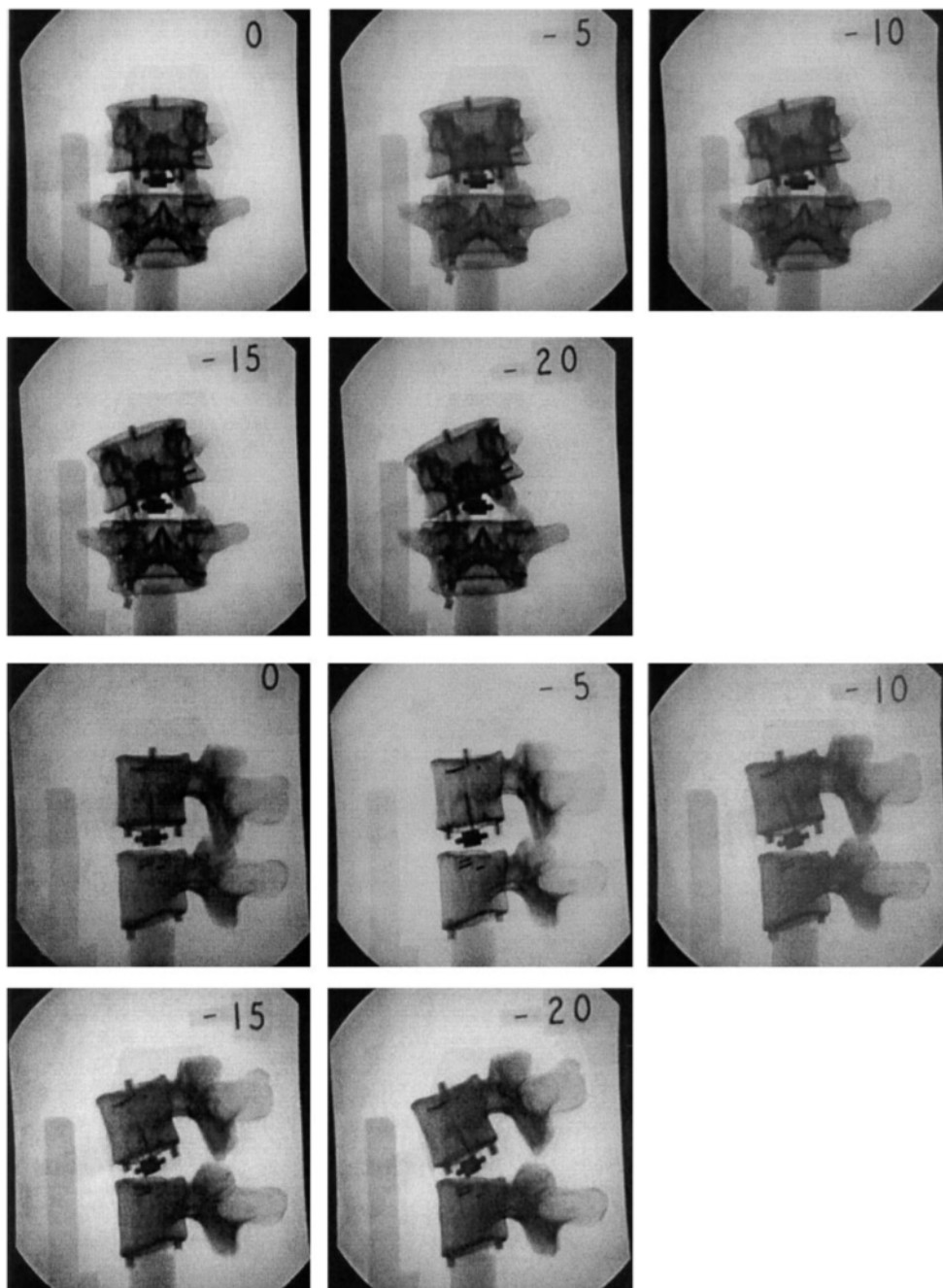


Fig. 9 Calibration model: fluoroscopic images (coronal and sagittal)

Each image was composed of 512 by 512 pixels (1 pixel = 0.25 mm) and 256 grey levels. The coronal sequence consists of the images CorL0, CorL5, CorL10, CorL15, CorL20. The

sagittal sequence consists of the images SagL0, SagL5, SagL10, SagL15, SagL20. The numbers at the end of the file name correspond to the rotation angle of the vertebra L3 with respect to the vertebra L4 in the model. The experiments carried out considered images CorL0 and SagL0 as references for the coronal and sagittal sequence respectively. All the kinematic parameters were computed with respect to the reference images.

The four landmarks were manually selected on each of the vertebral body corners of the reference images. Each vertebral template was then automatically enlarged by 15% of the mean dimension of the polygon formed by the landmarks in order to include a part of the surrounding image with the vertebral body (Fig. 4).

The kinematic parameters (intervertebral angle and ICR) were computed from two landmarks in conjunction with the rigid body model; for convenience the upper landmarks UL – UR were employed (see Section 3.2). Using the repetitive computation described in Section 2.7, a distribution of measurements was produced for each parameter. The means and the standard deviations of the results are presented, the mean giving a

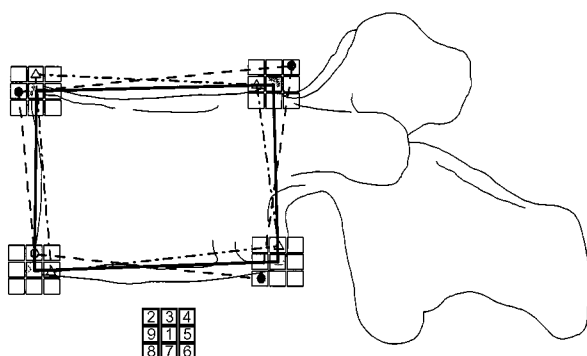


Fig. 10 Repeatability and sensitivity of the measurements: extended input data set and different combinations of the inputs

Table 1 Mean values and standard deviations of the computed distribution of intervertebral angles (coronal and sagittal image sequences)

| Preset angle, deg | Coronal | | Sagittal | |
|-------------------|-----------|---------|-----------|---------|
| | mean, deg | SD, deg | mean, deg | SD, deg |
| 5 | 5.2 | 0.08 | 5.1 | 0.08 |
| 10 | 10.4 | 0.10 | 10.1 | 0.15 |
| 15 | 15.3 | 0.12 | 15.8 | 0.16 |
| 20 | 20.6 | 0.24 | 20.8 | 0.16 |

measure of accuracy and the standard deviation a measure of repeatability.

Table 1 shows the results obtained for intervertebral angle estimation using the coronal and sagittal image sequences of the calibration model. The means are calculated to the nearest 0.1° and the standard deviations to the nearest 0.01° .

It can be seen in Table 1 that the calculated means are within $\pm 1^\circ$ of the preset angle, i.e. within the error margins imposed by the model (see Section 2.6). The small apparent errors in angle suggest a small systematic error in the model, over which we had no control for this study. However, the standard deviations can be seen to be always less than 0.3° , demonstrating good repeatability.

Table 2 shows the X and Y co-ordinates for the intervertebral centre of rotation.

Table 2 Mean values and standard deviations of the computed distribution of intervertebral ICR (coronal and sagittal image sequences)

| Preset angle | Coronal | | | | Sagittal | | | |
|--------------|---------|------|-------|------|----------|------|-------|------|
| | X | | Y | | X | | Y | |
| | mean | SD | mean | SD | mean | SD | mean | SD |
| 5 | 215.2 | 0.88 | 236.4 | 2.82 | 195.1 | 0.82 | 228.8 | 3.13 |
| 10 | 215.7 | 0.62 | 235.6 | 1.29 | 195.8 | 0.72 | 225.8 | 1.77 |
| 15 | 212.0 | 0.75 | 232.5 | 0.91 | 198.6 | 0.71 | 228.6 | 0.98 |
| 20 | 215.1 | 0.77 | 231.1 | 1.02 | 196.1 | 0.52 | 229.9 | 0.76 |
| Expected | 216 | | 231 | | 199 | | 229 | |

To visually appreciate the location of the ICRs obtained, they are plotted superimposed onto the reference frames. Figs 11a and 11b show coronal and sagittal views of the model, together with enlargements of these images to focus on the universal joint. The pixels corresponding to the mean values of the computed ICRs are plotted as white dots, together with ± 1 SD (as white lines), along the x and y directions.

Table 3 shows the ICRs errors computed as distances, expressed in millimetres, between the mean values of the results and the expected co-ordinates, corresponding to the centre of the universal joint (represented as a grey cross in Fig. 11).

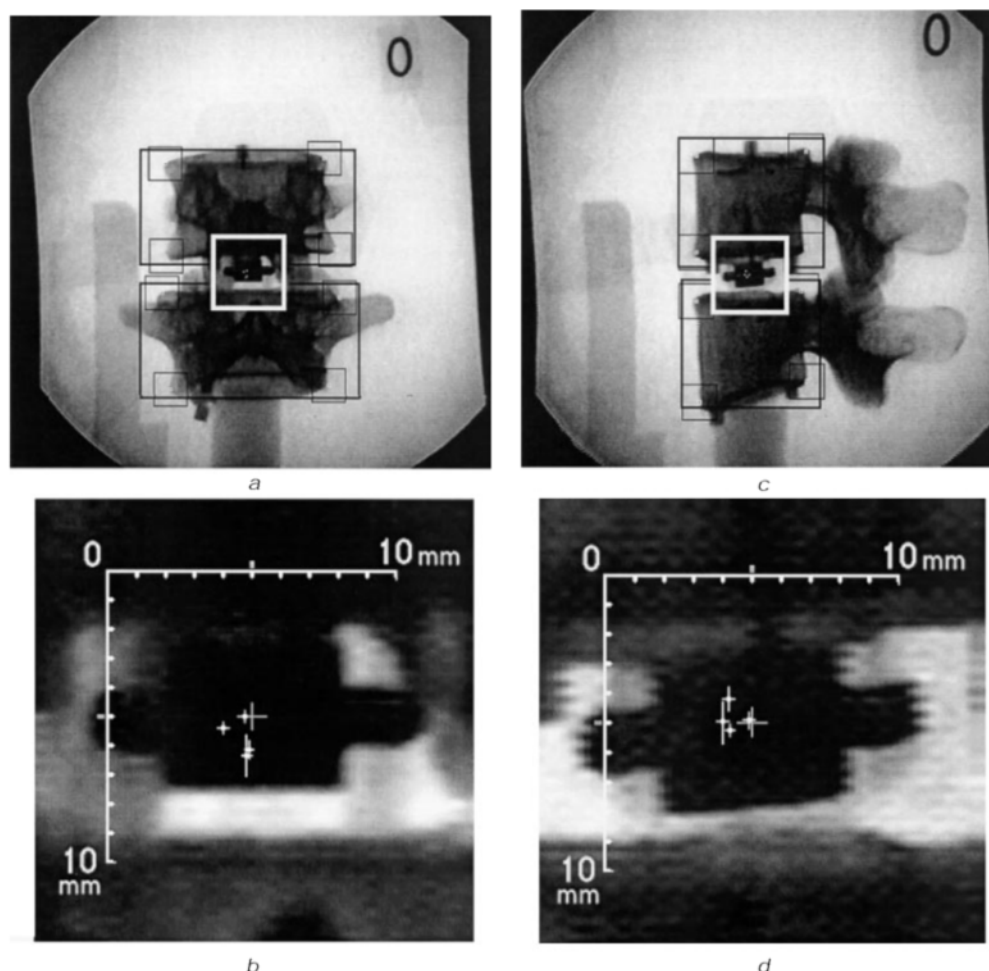


Fig. 11 (a) and (c) Reference images for the coronal and sagittal sequence: the selected landmarks (white dots), the vertebral templates (thick black line) and the landmark templates (thin black line) are superimposed. The white rectangle represents the area around the universal joint which is enlarged in (b) and (d). (b) and (d) Enlargement of the reference images centred around the universal joint (which appears as a rectangular dark area). The centre of the joint (expected location of the ICRs) is represented as a grey cross. The computed ICRs are represented as white dots, while horizontal and vertical white bars represent ± 1 SD. A scale (in white), marked in millimetres, helps

Table 3 Error distances between computed ICR means and expected values

| Preset angle | Coronal | Sagittal |
|--------------|--------------------|--------------------|
| | distance error, mm | distance error, mm |
| 5 | 1.4 | 1.0 |
| 10 | 1.2 | 1.1 |
| 15 | 1.1 | 0.2 |
| 20 | 0.2 | 0.7 |

3.2 Different choices of landmark pairs

Since only two points are necessary to identify a rigid body undertaking planar motion, the four vertebral landmarks can generate six different pairs. Each pair of landmarks shows different properties with respect to errors, according to the considerations expressed in Section 2.5.3. However, in this case, the relative positions of the landmark pairs with respect to the ICR do not vary significantly. In addition, the rigidity restoration procedure ensures invariance of the mutual positions of the landmarks, and the kinematic parameters computed are robust with respect to the choice of landmark pair (BIFULCO, 1998).

3.3 Example of analysis of *in vivo* images and presentation of the results

Fig. 12 shows an example of the application of the algorithm to the analysis of *in vivo* images and of the presentation of the results to the physician. The kinematic parameters computed for two subsequent images, extracted from a sequence depicting an extension movement of a patient, are displayed superimposed onto the second image. The segment L3–L4 is analysed. The distribution of the computed intervertebral ICRs (located at disc

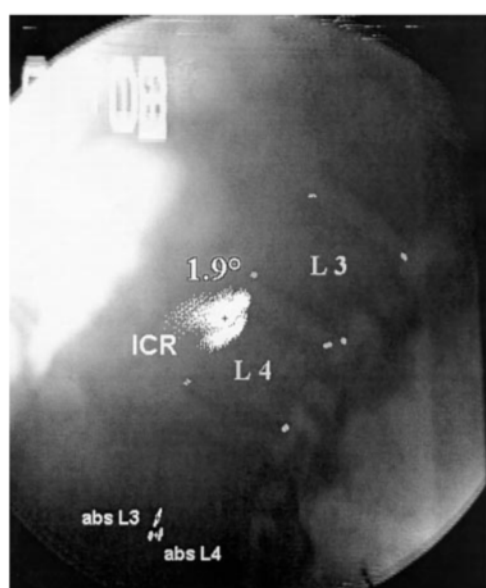


Fig. 12 Presentation of the kinematic parameters to the physician. Image extracted from a sagittal fluoroscopic sequence relative to a patient executing an extension movement. The mean intervertebral angle and the ICRs distribution relative to the L3–L4 segment, are represented. The absolute centres of rotation (with respect to the fluoroscope) of L3 and L4 are also displayed for comparison

level, slightly anteriorly), is represented in white (the mean value is represented as a black cross); the mean intervertebral angle (1.9°) is also displayed. The absolute values of the centre of rotation (with respect to the fluoroscope) of L3 (white) and L4 (10% grey) are also displayed for comparison. They both appear, very close to each other, at the bottom left of the image, approximately anteriorly and superiorly with respect to the sacrum.

4 Conclusions and discussion

This work proposes a methodology for estimating intervertebral kinematic parameters by extrapolating from vertebral landmark co-ordinates which are automatically identified throughout a digitised sequence of fluoroscopic images of the human spine *in vivo*. The procedure for recognition of the position of a vertebra is based upon cross-correlation of images, which is robust with respect to the high amount of noise typical of fluoroscopic images. This method constitutes an alternative to the tedious and imprecise manual selection of landmarks, providing an objective quantification of *in vivo* intervertebral kinematics. The algorithm developed provides the computation and visualisation of the kinematic parameters for diagnostic purposes.

The analysis of errors, performed by means of the calibration model, suggests that this method improves the reliability and the accuracy of intervertebral kinematics calculation. From the model images, the intervertebral angle can be measured to within 1° and the centre of rotation to within 2 mm. Analysis of the repeatability and sensitivity of the measurement by means of the iterative computation of the kinematic parameters, involving neighbouring pixels surrounding the landmarks, can be routinely utilised to provide an indication about the accuracy of each measurement for diagnosis. In particular, the mean values can be used to estimate the kinematic parameters and the standard deviations to indicate the repeatability of the measurements. In addition, this procedure reduces the influence of the intervention of the operator who has to select only the vertebral landmarks from the first image of the sequence.

From the analysis of the results it appears that that no significant differences appear from using different pairs of landmarks to compute the kinematic parameters. The mean values and the standard deviations of all the distributions remain very stable and this is considered to be a result of the rigidity constraint. Further discussion of the choice of landmarks is found in PANJABI (1979) and in PANJABI *et al.* (1992). It would be worth investigating in detail the effect of a possible propagation of kinematic errors during the processing of an images sequence.

The kinematic parameters here adopted to describe intervertebral motion are the intervertebral angle and the instantaneous centre of rotation, widely used in previous studies. However, this representation of the motion suffers from the difficulty of describing pure translation and/or small degrees of rotation. It would be useful, in future, to combine and integrate the use of other kinematic parameters to overcome such shortcomings (MUGGLETON and ALLEN, 1998). Moreover, the motion analysis is performed step-wise (frame by frame). Other techniques, such as the interpolation (e.g. using spline functions) of the landmark trajectories, could be evaluated to provide a continuous description of the motion.

A systematic analysis of *in vivo* fluoroscopic lumbar sequences of healthy volunteer subjects has begun using the proposed analysis method to provide reference information useful for clinical applications. Future work will concentrate

on the classification of asymptomatic and pathological patterns of kinematic parameters.

Acknowledgments—The authors are very grateful to Dr Alan Breen and colleagues at the Anglo-European College of Chiropractic, Bournemouth for their help and fruitful discussions.

The authors wish to thank the British Council – CRUI (British–Italian Collaboration in Research and Higher Education) for funding part of the research. Thanks go also to the Italian Ministry of Research and University MURST.

References

- AMEVO, B. (1991): 'Instantaneous axis of rotation of the typical cervical motion segments'. PhD thesis, University of Newcastle, Newcastle, Australia
- AMEVO, B., WORTH, D., and BOGDUK, N. (1991): 'Instantaneous axis of rotation of the typical cervical motion segments: a study in normal volunteers', *Clin. Biomech.*, **6**, pp. 111–117
- AN, H. S., HAUGHTON, V. M., LIM, T. H., HONG, J., NOWICKI, B., YOU, L., and YOSHIDA, H. (1996): 'The relationship between disc degeneration and kinematics characteristics of the lumbar spine motion segment'. Proceedings of the 11th Annual Conference of the North American Spine Society, 23–26 October 1996
- AUBIN, C. E., DANSERAU, J., PETIT, Y., PARENT, F., DE GUISE, J. A., and LABELLE, H. (1998): 'Three-dimensional measurement of wedged scoliotic vertebrae and intervertebral disks', *Eur. Spine J.*, **7**, pp. 59–65
- BAKKE, S. N. (1931): 'Roentgenologische Beobachtungen uber die Bewegungen de Wirbelsaule', *Acta Radiol. Suppl.*, 123
- BIFULCO, P., ALLEN, R., DELLA FERA, A., DE STEFANO, A., MAGLIULO, R., and BREEN, A. C. (1995): 'Automatic recognition of vertebral landmarks using videofluoroscopic images: an alternative for spine kinematics'. Proceedings of BIOMED '95 Simulation in Biomedicine, Milan, Italy, 21–23 June 1995
- BIFULCO, P., CESARELLI, M., SANSONE, M., ALLEN, R., and BRACALE, M. (1997): 'Fluoroscopic analysis of intervertebral lumbar motion: a rigid model fitting technique'. Proceedings of the World Congress on Medical Physics and Biomedical Engineering, Nice 14–19 September 1997
- BIFULCO, P. (1998): 'Analysis of intervertebral kinematics using fluoroscopic image sequences'. PhD thesis, University of Naples, Italy
- BOGDUK, N., AMEVO, B., and PEARCY, M. (1995): 'A biological basis for instantaneous centre of rotation of the vertebral column', *J. Eng. Med.*, **209**, pp. 177–183
- BREEN, A., ALLEN, R., and MORRIS, A. (1989): 'Spine kinematics: a digital videofluoroscopic technique', *J. Biomed. Eng.*, **11**, pp. 224–228
- BREEN, A. C. (1991): 'The measurement of the kinematics of the human spine using videofluoroscopy and image processing'. PhD thesis, University of Southampton, Southampton
- BREEN, A. C., BRYDGES, R., NUNN, H., KAUSE, J., and ALLEN, R. (1993): 'Quantitative analysis of lumbar spine intersegmental motion', *Eur. J. Physical Med. Rehab.*, **3**, pp. 182–190
- BROWN, B., BURNSTEIN, A., NASH, C., and SCHOCK, C. (1976): 'Spinal analysis using a three dimensional radiographic technique', *J. Biomech.*, **9**, pp. 355–365
- CHOLEWICKI, J., MCGILL, S., WELLS, B., and VERNON, H. (1991): 'Method for measuring vertebral kinematics from videofluoroscopy', *Clin. Biomech.*, **6**, pp. 73–78
- CHOLEWICKI, J., and MCGILL, S. M. (1992): 'Lumbar posterior ligament involvement during extremely heavy lifts estimated from fluoroscopic measurements', *J. Biomech.*, **25**, pp. 17–28
- DIMNET, J., FISCHER, L. P., GONON, G., and CARRET, J. P. (1978): 'Radiographic studies of lateral flexion in the lumbar spine', *J. Biomech.*, **11**, 143–150
- DITTMAR, O. (1929): 'Die saggital- und lateralflexorische Bewegung der menschlicher Lendewirbelsaule in Roentgenbild', *Z. f. d. ges. Anat.*, **92**, 644–667
- FICK, R., and STRASSER, H. (1913): 'Lehrbuch der muskel und Gelenk Mechanik' (Springer, Berlin)
- FRANKEL, V., and BURSTEIN, A. (1974): 'Biomechanics of the locomotor system, *Medical engineering in research. Year book*' (Medical Publisher Inc.), pp. 505–515
- FRIBERG, O. (1987): 'Lumbar instability: a dynamic approach by traction compression radiography', *Spine*, **12**, pp. 119–129
- GERTZBEIN, S. D., SELIGMAN, J., HOLTBY, K., CHAN, K. H., KAPASOURI, A., and CRUIKSHANK, B. (1985): 'Centroid patterns and segmental instability in degenerative disk disease', *Spine*, **4**, pp. 257–261
- GIANTURCO, C. (1944): 'A roentgen analysis of the motion of the lower lumbar vertebrae in normal individuals and in patient with low back pain', *Am. J. Roentgend.*, **52**, pp. 261
- HUANG, T. S., and NETRAVALI, A. N. (1994): 'Motion and structure from feature correspondences: a review' *Proc. IEEE*, **82**, 252–268
- JAIN, A. K. (1989): 'Fundamentals of digital image processing' (Prentice Hall International)
- KINZEL, G. L., HALL, A. S., and HILLBERRY, B. M. (1972): 'Measurements of the total motion between two body segments – I. Analytical development', *J. Biomech.*, **5**, pp. 93–105
- LYSELL, E. (1969): 'Motion in the cervical spine', *Acta Orthop. Scand.*, Suppl. 123
- MUGGLETON, J. M., and ALLEN, R. (1997): 'Automatic location of vertebrae in digitized videofluoroscopic images of the lumbar spine', *J. Med. Eng. Phys.*, **19**, pp. 77–89
- MUGGLETON, J. M., and ALLEN, R. (1998): 'Insights into the measurement of vertebral translation in the sagittal plane', *J. Med. Eng. Phys.*, **20**, pp. 21–32
- PAGE, W. H., and MONTEITH, W. (1992): 'Bone movement analysis from computer processing of X-ray cinematic video images'. Proceedings of the 4th International Conference on Image Processing, IEEE, 354, pp. 381–384
- PAGE, W. H., MONTEITH, W., and WITHEHEAD, L. (1993): 'Dynamic spinal analysis – fact or fiction', *Chiropractic J. Australia*, **23**, pp. 82–85
- PANJABI, M., and WHITE, A. (1971): 'A mathematical approach for three-dimensional analysis of the mechanics of the spine', *J. Biomech.*, **4**, pp. 203–211
- PANJABI, M. (1973): 'Three-dimensional mathematical model of the human spine structure', *J. Biomech.*, **6**, pp. 671–680
- PANJABI, M. (1979): 'Centers and angles of rotation of body joints: a study of errors and optimization', *J. Biomech.*, **12**, pp. 911–920
- PANJABI, M., CHANG, D., and DVORAK, J. (1992): 'An analysis of errors in kinematics parameters associated with in vivo functional radiographs', *Spine*, **2**, pp. 200–205
- PEARCY, M., and TIBREWAL, S. (1984): 'Axial rotation and lateral bending in the normal lumbar spine measured by three-dimensional radiography', *Spine*, **6**, pp. 582–587
- PEARCY, M., PORTEK, I., and SHEPHERD, J. (1984): 'Three-dimensional X-ray analysis of normal movement in the lumbar spine', *Spine*, **3**, pp. 294–297
- PEARCY, M. (1985): 'Stereoradiography at lumbar spine motion', *Acta Orthop. Scand.*, Suppl. 212, Munksgaard, Copenhagen
- PEARCY, M. (1986): 'Measurement of back and spinal mobility', *Clin. Biomech.*, **1**, pp. 44–51
- PEARCY, M., and BOGDUK, N. (1988): 'Instantaneous axes of rotation of the lumbar intervertebral joints', *Spine*, **13**, pp. 1033–1041
- ROLANDER, S. D. (1966): 'Motion of the lumbar spine with special reference to the stabilizing effect of posterior fusion', *Acta Orthop. Scand.*, Suppl. 90
- SIMONIS, C. (1994): 'Parallel calculation and analysis of spine kinematics using videofluoroscopy and image processing'. PhD thesis, University of Southampton, Southampton
- SIMONIS, C., ALLEN, R., and BREEN, A. (1994): 'Rigid model fitting technique: an alternative in the selection of landmarks on spinal images'. Proceedings of the fifth Symposium on Biomedical Engineering, Santiago de Compostela, **2**, pp. 103–104
- STEFFEN, T., RUBIN, R. K., BARAMKI, H. G., ANTONIOU, J., MARCHESI, D., and AEBI, M. (1997): 'A new technique for measuring lumbar segmental motion in vivo', *Spine*, **22**, pp. 156–166

- TANZ, S. S. (1953): 'Motion of the lumbar spine', *Am. J. Roentgend.*, **69**, pp. 399–412
- TODD, T. W., and PYLE, I. S. (1928): 'A quantitative study of the vertebral column by direct roentgenologic methods', *Amer. J. Phys. Anthropol.*, **12**, pp. 321
- VAN MAMEREN, H. (1988): 'Motion patterns in the cervical spine'. PhD thesis, University of Limburg, Dept. of Anatomy and Embriology, The Netherlands
- VAN MAMEREN, H., DRUKKER, J., SANCHES, H., and BEURSGENS, J. (1990): 'Cervical spine motion in the sagittal plane (I) range of motion of actually performed movements, and X-ray cinematographic study', *Eur. J. Morphology*, **28**, pp. 47–68
- VAN MAMEREN, H., SANCHES, H., BEURSGENS, J., and DRUKKER, J. (1992): 'Cervical spine motion in the sagittal plane (II) position of segmental averaged instantaneous centers of rotation—a cineradiographic study', *Spine*, **17**, pp. 467–474
- WEBER, E. H. (1827): 'Anatomisch-physiologisch Unter such ungen ubereinige Einrichtungen im Mechanismus der Menschlichen Wirbelsaule', *Arch. Anat. Physiol. Joahn Fr. Meckel*, pp. 240–271
- WHITE, A. (1969): 'Analysis of the thoracic spine in man', *Acta Orthop. Scand.*, **III**, Suppl. 123

Authors' biographies

PAOLO BIFULCO received his Laurea in Electronic Engineering from the University of Naples "Federico II" in 1993. In 1991–92 he attended the "European Course on Biomedical Engineering and Medical Physics" at the University of Patras. In 1994, he was a Research Assistant at the University of Southampton, UK. He received his PhD in Bioengineering from the University of Naples "Federico II" in 1998. He is currently a Research Fellow at the Department of Electronic Engineering and Telecommunication of the University of Naples, where he has worked since 1992. His main research activities are in the field of biomedical signal and image processing.

MARIO CESARELLI received his Degree in Electronic Engineering from the University of Naples in 1979 and Postgraduate Specialisation in Biomedical Technologies from the University of Naples. Since 1992 he has been an Associate Professor in Biomedical Engineering (Biomedical Signal and Image Processing). His main fields of scientific interest are biosignal and image analysis, biomedical instrumentation, health care information systems, and health technology assessment.

ROBERT ALLEN holds a Personal Chair in Biodynamics and Control at the Institute of Sound and Vibration Research (ISVR), University of Southampton, UK. Following training in the machine tool industry and a period as a numerical control programme engineer, he studied at the University of Leeds and graduated with BSc (Hons) in Control Engineering and was awarded a PhD for research on modelling the dynamic characteristics of neural receptors. This was followed by postdoctoral positions at the University of Leeds (Dept. Anaesthesia) on monitoring intracranial pressure of severely head-injured patients to prevent secondary brain damage, and at the Welsh National School of Medicine, Cardiff (Dept. Anaesthetics) on a parameter estimation approach to noninvasive measurement of cardiac output. He moved to the University of Southampton (Faculty of Medicine) in 1984 to a newly created position as Lecturer in Biocomputation, and from there to the Department of Mechanical Engineering in 1985 as Lecturer and Senior Lecturer in Control Engineering and to the ISVR in 1997. His research interests are currently focused on the robust control of unmanned, underwater vehicles and on the development and application of signal processing techniques for biomedical systems analysis. Particular interests include functional electrical stimulation for paraplegic cycling, efficient estimation of auditory evoked potentials for assessment of hearing and of depth of anaesthesia, cerebral hydrodynamic modelling and noninvasive assessment of intracranial compliance, and processing of fluoroscopic images for measurement of spine kinematics.

MARIO SANSONE was born in Naples, Italy, in 1970. He received his Degree in Electronic Engineering from the University of Naples in 1997. He is currently working towards a PhD in Biomedical Engineering at the University of Naples, where he has worked, within the Department of Electronic Engineering and Telecommunication, since 1997. His interests are in the area of biomedical signal and image processing.

MARCELLO BRACALE was born in Naples, Italy, in 1939. He received his Degree in Electronic Engineering from the University of Naples in 1965 and Postgraduate Specialisation in Biomedical Technologies from the University of Bologna. Since 1976 he has been a Full Professor in Applied Electronics, and from 1980 he has been a Full Professor in Biomedical Engineering. His main fields of scientific and professional interest are electronic and biological instrumentation, biosignal and data analysis, health care systems and management, and telemedicine.